

Scaling approach to related disordered stochastic and free-fermion models

R. J. Harris^{1, 2, *} and R. B. Stinchcombe^{1, †}

¹*Rudolf Peierls Centre for Theoretical Physics, University of Oxford, 1 Keble Road, Oxford, OX1 3NP, UK*

²*Institut für Festkörperforschung, Forschungszentrum Jülich, 52425 Jülich, Germany*

(Dated: June 22, 2006)

Motivated by mapping from a stochastic system with spatially random rates, we consider disordered non-conserving free-fermion systems using a scaling procedure for the equations of motion. This approach demonstrates disorder-induced localization acting in competition with the asymmetric driving. We discuss the resulting implications for the original stochastic system.

PACS numbers: 02.50.Ey, 05.50.+q, 05.40.-a, 75.10.Jm

I. INTRODUCTION

The role of disorder in stochastic non-equilibrium systems is a topic of much recent interest (see e.g., [1, 2, 3, 4, 5] and references therein). This is exemplified by studies of the asymmetric simple exclusion process (ASEP), a one-dimensional lattice gas model exhibiting a phase transition for open boundary conditions. The effect of quenched particle-disordered hop rates in this system was investigated in, e.g., [6, 7, 8] and the case of quenched spatial disorder has been clarified by a number of works (see, e.g., [2, 9, 10]) including via a linearization transformation and scaling approach [11].

In this paper we study a related non-equilibrium model with applications in catalysis—the partially asymmetric exclusion process combined with deposition and evaporation of dimers (or equivalently pair annihilation and creation). Studies of the pure model e.g., [12, 13, 14] suggest that for non-vanishing adsorption and desorption rates, even with open boundary conditions [15, 16], there is no steady-state phase transition (unlike the ASEP). However, the effect of disorder on both steady-state properties (such as the density) and dynamics is still of interest

Here we demonstrate that, for spatially disordered rates obeying a particular condition, one can approach this problem via a powerful mapping to free-fermion systems. Therefore we study the equivalent disordered free-fermion system by applying a scaling procedure [11, 17] to the (linear) equations of motion. This work thus contributes to understanding of disordered free-fermions as well as illustrating a potential way to make progress with the disordered stochastic model.

The plan of the rest of the paper is as follows. In Sec. II we define our model, introduce the quantum Hamiltonian formalism and demonstrate the free-fermion reduction for a particular choice of disorder. We also discuss the known pure results. In Sec. III, we derive the coupled equations of motions for the disordered free-fermion case. Then, in Sec. IV we exploit the fact that these equations are linear

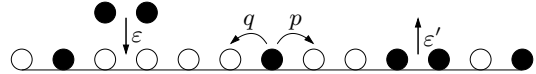


FIG. 1: Partially asymmetric exclusion process with dimer evaporation and deposition (pure model). Filled circles indicate particles; open circles denote vacancies.

to apply scaling techniques based on those in [11, 17]. As in those works, we find that disorder induces localization effects and in Sec. V we tentatively discuss the consequences for the original stochastic system. Finally, Sec. VI contains conclusions and suggestions for future work.

II. MODEL AND MAPPINGS

Let us start by considering the pure partially asymmetric exclusion process with dimer evaporation and deposition, shown schematically in Fig. 1. Subject to the exclusion constraints, particles hop to the right (left) with rate p (q), and pairs of particles are deposited (evaporated) with rate ε (ε'). This provides a simple model for adsorption-desorption processes and catalytic surface reactions.

In the special case $p + q = \varepsilon + \varepsilon'$, the system can be mapped via a Jordan-Wigner transformation [18] and a Bogoliubov-Valatin transformation [19, 20] to a free-fermion problem and hence solved exactly [12, 13, 21, 22]. The results are of more general significance since, by duality transformations and spin rotations, the quantum Hamiltonian can also be mapped to other stochastic systems [14, 23], including some which are experimentally realizable [24]. A subcase is $p = q = \varepsilon = \varepsilon'$ which maps to the Ising model and so is well understood [22].

The aim of the present work is to study the spatially-disordered version of this model, with rates p_l , q_l , ε_l and ε'_l for processes on the bond between sites l and $l + 1$. In this section we demonstrate that the mapping to free-fermions is still valid in the case where $p_l + q_l = \varepsilon_l + \varepsilon'_l$ for each l .

The generalized pair process parameterized by p_l , q_l , ε_l and ε'_l can be conveniently represented using the quan-

*Electronic address: r.harris@fz-juelich.de

†Electronic address: stinch@thphys.ox.ac.uk

tum Hamiltonian formalism [25]. In this approach one defines a probability vector $|P\rangle = \sum_n P_n |n\rangle$ with $|n\rangle$ the basis vector associated with the particle configuration $n = (n_1, n_2, \dots, n_L)$ and P_n the probability measure on the set of all such configurations. $|P\rangle$ obeys the normalization condition $\langle s|P\rangle = 1$ where $\langle s| = \sum_n \langle n|$ and $\langle n|n'\rangle = \delta_{n,n'}$. Within this formalism the master equation for the time evolution resembles a Schrödinger equation

$$\frac{d}{dt} |P(t)\rangle = -H |P(t)\rangle \quad (1)$$

with

$$\begin{aligned} H = & - \sum_l [p_l \sigma_l^- \sigma_{l+1}^+ + q_l \sigma_l^+ \sigma_{l+1}^- + \varepsilon_l \sigma_l^+ \sigma_{l+1}^+ + \varepsilon'_l \sigma_l^- \sigma_{l+1}^- \\ & - \frac{1}{4}(p_l + q_l + \varepsilon_l + \varepsilon'_l) + \frac{1}{4}(-p_l + q_l + \varepsilon_l - \varepsilon'_l) \sigma_l^z \\ & + \frac{1}{4}(p_l - q_l + \varepsilon_l - \varepsilon'_l) \sigma_{l+1}^z + \frac{1}{4}(p_l + q_l - \varepsilon_l - \varepsilon'_l) \sigma_l^z \sigma_{l+1}^z]. \end{aligned} \quad (2)$$

Here the “spin-flip” operators σ^\pm correspond to particle creation and annihilation processes while the projection operators σ_z are needed to account for the probability that configurations do not change. Conservation of probability imposes the condition

$$\langle s|H = 0. \quad (3)$$

Note that the general four-parameter model defined by (2) contains many other important models as sub-cases, e.g., the ASEP ($q_l = \varepsilon_l = \varepsilon'_l = 0$), symmetric diffusion ($p_l = q_l, \varepsilon_l = \varepsilon'_l = 0$), etc. Further progress depends on what boundary terms are imposed and how tractable the resultant quantum spin model is. In particular, a Jordan-Wigner transformation to fermion operators c_l^\dagger, c_l gives both an easily treatable quadratic part (arising from $\sigma^\pm \sigma^\pm$ and σ_z terms) and a more difficult quartic part (from the $\sigma_z \sigma_z$ terms). The quartic terms will clearly be zero for the special case

$$p_l + q_l = \varepsilon_l + \varepsilon'_l \quad (4)$$

and this gives the disordered free-fermion model which will be explored in more detail in the remainder of this paper.

For this particular case, we now outline the details of the transformation to fermion operators (compare Grinberg *et al.* [22] for the pure model). Writing σ_z in terms of $\sigma^+ \sigma^-$ and imposing periodic boundary conditions, Eq. (2) becomes

$$\begin{aligned} H_{\text{FF}} = & - \sum_l [p_l \sigma_l^- \sigma_{l+1}^+ + q_l \sigma_l^+ \sigma_{l+1}^- + \varepsilon_l \sigma_l^+ \sigma_{l+1}^+ + \varepsilon'_l \sigma_l^- \sigma_{l+1}^- \\ & + (p_{l-1} - p_l + \varepsilon_l - \varepsilon'_{l-1}) \sigma_l^+ \sigma_l^- - \varepsilon_l]. \end{aligned} \quad (5)$$

Then applying the usual Jordan-Wigner transformation [18]

$$\sigma_l^+ = c_l^\dagger \exp \left(i\pi \sum_{j < l} c_j^\dagger c_j \right) \quad (6)$$

$$\sigma_l^- = \exp \left(-i\pi \sum_{j < l} c_j^\dagger c_j \right) c_l, \quad (7)$$

yields the Hamiltonian in terms of fermion operators¹

$$\begin{aligned} H_{\text{FF}} = & \sum_l [p_l c_l c_{l+1}^\dagger - q_l c_l^\dagger c_{l+1} - \varepsilon_l (c_l^\dagger c_{l+1}^\dagger - 1) \\ & + \varepsilon'_l c_l c_{l+1} - (p_{l-1} - p_l + \varepsilon_l - \varepsilon'_{l-1}) c_l^\dagger c_l]. \end{aligned} \quad (8)$$

The study of the disordered free-fermion Hamiltonian (8) is the central aim of this paper; we now digress to summarize the known pure results.

In the pure case one can exploit translational invariance via a Fourier transformation and then use a Bogoliubov-type similarity transformation [19, 20] (well defined only for ε and ε' non-zero) to diagonalize the Hamiltonian. The details are given in [12, 22]; here we simply quote the resulting Hamiltonian:

$$H_{\text{FF}} = \sum_k \lambda_k \xi_k^+ \xi_k, \quad (9)$$

with spectrum

$$\lambda_k = \varepsilon + \varepsilon' + (\varepsilon - \varepsilon') \cos k + i(p - q) \sin k. \quad (10)$$

The imaginary part of λ_k implies ballistic motion while the real part indicates that excitations decay with time constant $[\varepsilon + \varepsilon' + (\varepsilon - \varepsilon') \cos k]^{-1}$. For ε and ε' non-zero, the spectrum is gapped giving exponentially fast kinetics. By mapping back from this free-fermion model, one can obtain the steady-state density profile for the original pure stochastic problem. The result [22]

$$\rho_l = \frac{1}{1 + \sqrt{\varepsilon'/\varepsilon}}, \quad (11)$$

is in agreement with mean-field calculation (one can show that the system is spatially uncorrelated). Other works have calculated dynamic correlation functions [12, 13], shock evolution [26], persistence probability, etc. Note that non-steady-state properties of the stochastic system can be understood by mapping to the Glauber model [27] and treating the asymmetric hopping as biased diffusion of domain walls [28].

¹ If the total number of fermions, $\sum_l \sigma_l^+ \sigma_l^- = \sum_l c_l^\dagger c_l$, is even then the fermion operators must obey cyclic boundary conditions; in the odd subspace, anti-cyclic boundary conditions are required. See [22].

The simplest disordered scenario, the case of a single defect, produces the stochastic analogue of localized modes [29]. One might also expect to make progress for the case of dilution, by breaking the chain up into finite uniform sections (compare the treatment of the diffusion-only problem in [30]; a similar break-up into effective pure segments also occurs in [5]). In this paper we are chiefly interested in more general disordered cases where there is no translational invariance and so one can not utilize the usual Fourier and Bogliubov transformations. However, work by Merz and Chalker involving doubling the number of fermion operators [31], offers the possibility of using a type of a localized Bogliubov transformation followed by numerical calculation. Another potential way to make progress is to derive and work with the linear dynamic equations. We will pursue this latter approach in the next section.

III. EQUATIONS OF MOTION

Let us first consider the expectation value of a general observable X , i.e.,

$$\langle X \rangle(t) = \langle s | X | P \rangle. \quad (12)$$

where we use angular brackets to denote this stochastic average over histories. Using the “Schrödinger equation” (1) one sees that the time evolution of $\langle X \rangle$ is given by

$$\frac{\partial \langle X \rangle}{\partial t} = \langle [H, X] \rangle \quad (13)$$

with $[H, X]$ the usual commutator.

For the free-fermion Hamiltonian (8) we can use the fermion anti-commutation relations, together with the identity $[A, BC] = \{A, B\}C - B\{A, C\}$, to calculate the commutators $[c_j, H]$ and $[c_j^\dagger, H]$ and hence obtain coupled dynamic equations for the operators:

$$\frac{\partial c_j}{\partial t} = p_{j-1}c_{j-1} + q_jc_{j+1} - \varepsilon_{j-1}c_{j-1}^\dagger + \varepsilon_jc_{j+1}^\dagger \quad (14)$$

$$+ (p_{j-1} - p_j + \varepsilon_j - \varepsilon'_{j-1})c_j, \quad (15)$$

$$\frac{\partial c_j^\dagger}{\partial t} = -p_jc_{j+1}^\dagger - q_{j-1}c_{j-1}^\dagger + \varepsilon'_{j-1}c_{j-1} - \varepsilon'_jc_{j+1} \quad (16)$$

$$- (p_{j-1} - p_j + \varepsilon_j - \varepsilon'_{j-1})c_j^\dagger. \quad (17)$$

Note that due to the non-Hermicity of H these equations are not simply Hermitian conjugates of each other. The equations are linear thus raising the possibility of using scaling techniques like those in [11, 17]—this will be the subject of the next section.

As a preliminary to this scaling approach, we first assume that c_j and c_j^\dagger can be written as superpositions of

operators with exponential time dependence:

$$c_j = \sum_{\omega} \Gamma_j(\omega) e^{\omega t}, \quad (18)$$

$$c_j^\dagger = \sum_{\omega} \gamma_j(\omega) e^{\omega t}. \quad (19)$$

Substituting into Eqs. (15) and (17) and equating components with the same time dependence yields

$$(E_j - \omega)\Gamma_j = -p_{j-1}\Gamma_{j-1} - q_j\Gamma_{j+1} + \varepsilon_{j-1}\gamma_{j-1} - \varepsilon_j\gamma_{j+1}, \quad (20)$$

$$(E_j + \omega)\gamma_j = -p_j\gamma_{j+1} - q_{j-1}\gamma_{j-1} + \varepsilon'_{j-1}\Gamma_{j-1} - \varepsilon'_j\Gamma_{j+1}, \quad (21)$$

$$\text{with } E_j = (p_{j-1} - p_j + \varepsilon_j - \varepsilon'_{j-1}).$$

Note that for the pure case we can carry out a Fourier transformation by writing $\Gamma_j(\omega) = e^{-ikj}\Gamma_k$, $\gamma_j(\omega) = e^{-ikj}\gamma_k$. As expected, we then find that for each Fourier component, Eqs. (20) and (21) have solutions with $\omega = \lambda_k$ or $\omega = -\lambda_{-k}$, where λ_k is the pure spectrum (10). In other words the operators c_j and c_j^\dagger can be written as

$$c_j = \sum_k e^{-ikj}(\Gamma_k e^{\lambda_k t} + \Gamma'_k e^{-\lambda_{-k} t}), \quad (22)$$

$$c_j^\dagger = \sum_k e^{-ikj}(\gamma_k e^{\lambda_k t} + \gamma'_k e^{-\lambda_{-k} t}), \quad (23)$$

where

$$\gamma_k = i\Gamma_k \frac{\varepsilon'}{\varepsilon} \cot \frac{k}{2}, \quad (24)$$

$$\gamma'_k = -i\Gamma'_k \tan \frac{k}{2}. \quad (25)$$

This approach thus provides an alternative route to construct the Bogliubov transformation; note that we can obtain the Bogliubov angle from the relations (24) and (25).

For the more general disordered case, we can cast Eqs. (20) and (21) in the form of a transfer matrix mapping:

$$\begin{pmatrix} X_{j+1} \\ X_j \end{pmatrix} = \begin{pmatrix} W^{-1} & -W^{-1}V \\ 1 & 0 \end{pmatrix} \begin{pmatrix} X_j \\ X_{j-1} \end{pmatrix}, \quad (26)$$

where X_j is the column vector

$$X_j = \begin{pmatrix} \Gamma_j \\ \gamma_j \end{pmatrix}, \quad (27)$$

and V and W are the 2×2 matrices

$$V = \begin{pmatrix} -p_{j-1} & \varepsilon_{j-1} \\ \frac{\varepsilon_{j-1}}{E_j - \omega} & \frac{\varepsilon_{j-1}}{E_j - \omega} \end{pmatrix}, \quad (28)$$

$$W = - \begin{pmatrix} q_j & \varepsilon_j \\ \frac{q_j}{E_j + \omega} & \frac{\varepsilon_j}{E_j + \omega} \end{pmatrix}. \quad (29)$$

Note that the transfer matrix is a function of ω . In the pure case we expect to be able to recover both the spectrum and the Bogoliubov mixing angles by considering the nature of the eigenvalues (real versus complex) and their ratios; compare the simpler models treated in [32]. Analysing products of disordered transfer matrices then provides a way to investigate possible localization effects. This is a particularly attractive approach for simple models such as binary disorder. In the next section we develop instead, a general numerical scaling approach for arbitrary distributions of disorder in Eqs. (20) and (21).

IV. SCALING

A. Procedure

In the general disordered case it is not obvious how to solve Eqs. (20) and (21) explicitly but their form is reminiscent of an equation which appears in the disordered ASEP (in a mean-field description) after a linearizing (Cole-Hopf) transformation so we can develop a scaling method similar to the one used in that case [11] (compare again the original work of Pimentel and Stinchcombe [17]). For full generality we must allow each coefficient to scale differently [e.g., the coefficient of Γ_{j-1} in (20) can scale differently from the coefficient of γ_{j+1} in (21), even in the pure case]. So we perform a $b = 2$ dilation of the system using decimation on the following equations

$$(E_j - \omega)\Gamma_j = -p_{j,j-1}\Gamma_{j-1} - q_{j,j+1}\Gamma_{j+1} + \varepsilon_{j,j-1}\gamma_{j-1} - \tilde{\varepsilon}_{j,j+1}\gamma_{j+1}, \quad (30)$$

$$(\tilde{E}_j + \omega)\gamma_j = -\tilde{p}_{j,j+1}\gamma_{j+1} - \tilde{q}_{j,j-1}\gamma_{j-1} + \varepsilon'_{j,j-1}\Gamma_{j-1} - \tilde{\varepsilon}'_{j,j+1}\Gamma_{j+1}. \quad (31)$$

where we have extended the subscript notation for clarity. The resulting 10-parameter scaling equations are rather involved and are displayed for convenience in Appendix A.

We now test this scaling procedure on the pure model (Sec. IV B) before applying it to the disordered problem (Sec. IV C).

B. Pure model

We here demonstrate how the scaling of the equations of motion (30) and (31) reflects the known spectrum λ_k of the pure model (10). For definiteness we consider the case $\varepsilon > \varepsilon'$, $p \geq q$ throughout; the extension to other cases should be straightforward, since they are related by duality or space reflection.

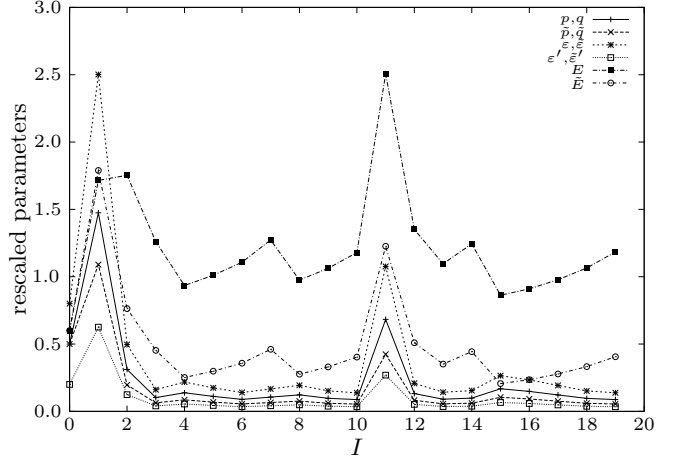


FIG. 2: Evolution of parameters in Eqs. (30) and (31) under $b = 2$ decimation. Pure case with $\omega = 0.41$ and starting parameter values $p = \tilde{p} = q = \tilde{q} = 0.5$, $\varepsilon = \tilde{\varepsilon} = 0.8$, $\varepsilon' = \tilde{\varepsilon}' = 0.2$, $E = \tilde{E} = 0.6$. Graph shows absolute magnitude of parameters against number of iterations I ; lines are provided as an aid to the eye. Chaotic behaviour is typical of scaling in the allowed band.

1. Non-biased case, $p = q$

For the pure case, if one starts with $p = \tilde{p} = q = \tilde{q}$, $\varepsilon = \tilde{\varepsilon}$, $\varepsilon' = \tilde{\varepsilon}'$, and by implication $E = \tilde{E}$, then the relationships $p = q$, $\tilde{p} = \tilde{q}$, $\varepsilon = \tilde{\varepsilon}$ and $\varepsilon' = \tilde{\varepsilon}'$ are preserved under scaling so one only needs to scale six independent parameters. We find two distinct types of scaling behaviour.

For $2\varepsilon' \leq \omega \leq 2\varepsilon$ the scaling parameters all evolve chaotically under scaling (see Fig. 2). In contrast for $\omega < 2\varepsilon'$ or $\omega > 2\varepsilon$, the “energies” E and \tilde{E} tend to constant values whereas the rescaled rates r (i.e., p , q , etc.) tend rapidly to zero inside an exponentially decaying envelope (see Fig. 3), i.e., $r(l) \sim f(l)e^{-l/\xi}$ where $l = 2^I$ is the distance between sites (I is the number of iterations) and ξ is a localization length. We also see this localized behaviour for all non-real ω .

Just as in the scaling of the Cole-Hopf-transformed mean-field ASEP [11] the localization length can be measured numerically from the exponential decay of the parameters. In Fig. 4 we plot the localization length obtained from the scaling of p , as a function of real frequency ω (localization lengths obtained from the other rates are found to be identical). These numerical results can be simply explained by reference to the pure spectrum for the symmetric case. The allowed band (real k) corresponds to the region $2\varepsilon' \leq \omega \leq 2\varepsilon$; here states are extended and the localization length is infinite. Frequencies outside this band correspond to a complex wave-vector $k + i\kappa$, i.e., localized states with localization length $\xi = 1/\kappa$. Indeed, from $\omega = \varepsilon + \varepsilon' + (\varepsilon - \varepsilon') \cos(k + i\kappa)$ we can obtain an analytical expression for the localization

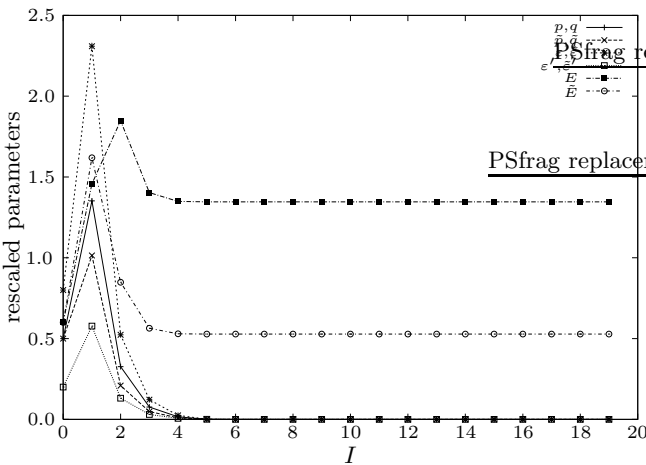


FIG. 3: Evolution of parameters in Eqs. (30) and (31) under $b = 2$ decimation. Pure case with $\omega = 0.39$ and starting parameter values $p = \tilde{p} = q = \tilde{q} = 0.5$, $\varepsilon = \tilde{\varepsilon} = 0.8$, $\varepsilon' = \tilde{\varepsilon}' = 0.2$, $E = \tilde{E} = 0.6$. Graph shows absolute magnitude of parameters against number of iterations I ; lines are provided as an aid to the eye. Rate parameters decay exponentially as a function of 2^I , as expected outside the allowed band.

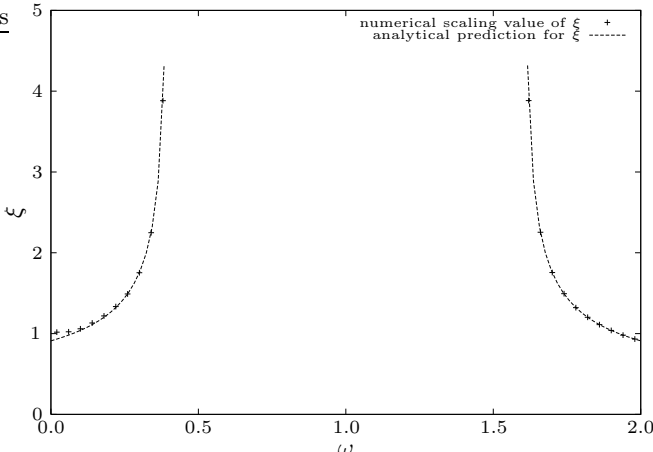


FIG. 4: Localization length ξ versus (real) frequency ω for pure case with $p = q = 0.5$, $\varepsilon = 0.8$, $\varepsilon' = 0.2$. ξ is effectively infinite in allowed band $0.4 < \omega < 1.6$. Crosses indicate data from numerical scaling of rate p ; dashed line is analytical prediction of Eq. (32).

length on the real- ω axis ($k = 0$ or $k = \pi$):

$$\xi = \left(\operatorname{arccosh} \left| \frac{\varepsilon' + \varepsilon - \omega}{\varepsilon' - \varepsilon} \right| \right)^{-1}. \quad (32)$$

This expression is shown as a dashed line in Fig. 4 and agreement with the numerics is excellent.

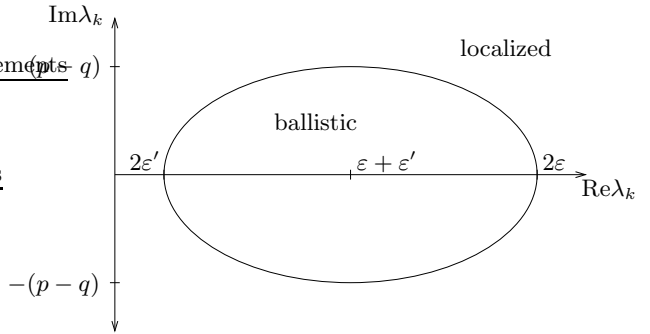


FIG. 5: $\operatorname{Im} \lambda_k$ versus $\operatorname{Re} \lambda_k$ for pure model (case $p > q$, $\varepsilon > \varepsilon'$). Solid ellipse represents allowed spectrum given by (10). Inside the ellipse equations of motion scale to ballistic limit $p/q \rightarrow \infty$; outside of ellipse is localized region.

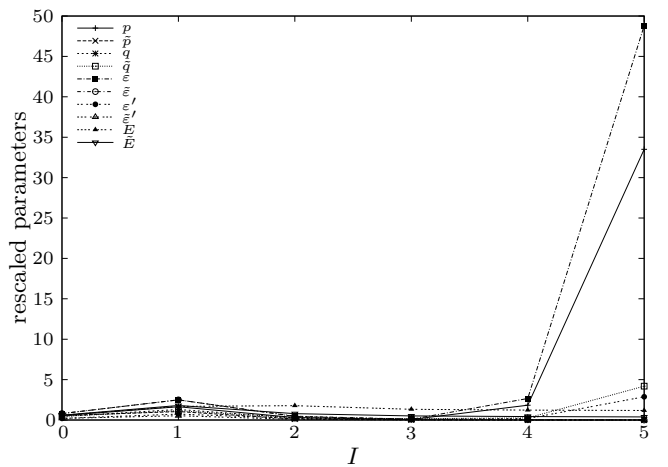


FIG. 6: Evolution of parameters in Eqs. (30) and (31) under $b = 2$ decimation (first few iterations). Pure case with $\omega = 0.41$ and starting parameter values $p = \tilde{p} = 0.55$, $q = \tilde{q} = 0.45$, $\varepsilon = \tilde{\varepsilon} = 0.8$, $\varepsilon' = \tilde{\varepsilon}' = 0.2$, $E = \tilde{E} = 0.6$. Graph shows absolute magnitude of parameters against number of iterations I ; lines are provided as an aid to the eye. Rates p , q , ε , ε' scale exponentially to infinity while \tilde{p} , \tilde{q} , $\tilde{\varepsilon}$, $\tilde{\varepsilon}'$ decay exponentially and “energies” E , \tilde{E} tend to constant values. This is typical of ballistic behaviour inside the allowed ellipse (for case $p > q$).

2. Biased case, $p \neq q$

In the pure biased case the allowed values of ω are given by λ_k of Eq. (10) with k real—an ellipse in complex k -space, see Fig. 5. For these values of ω we again find, as expected, that the scaling parameters all evolve chaotically under scaling. Outside this allowed ellipse we see localized states once more.

Inside the ellipse we see a new type of behaviour— E and \tilde{E} again tend to constant values, some of the rates scale exponentially to zero, whereas others grow exponentially to infinity (see Fig. 6). We argue that in this region the system is dominated by the ballistic motion

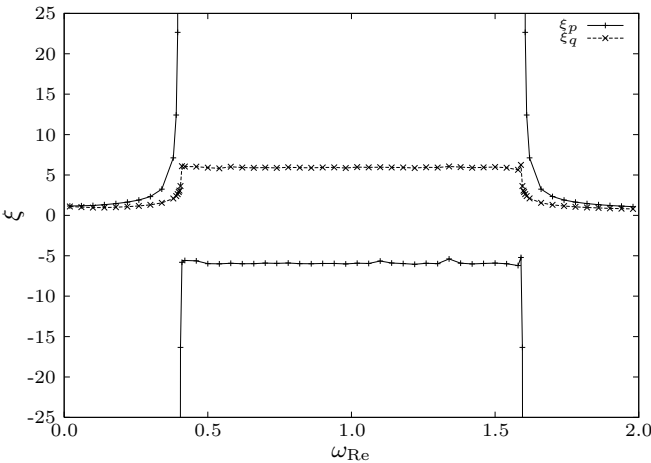


FIG. 7: Numerical localization lengths ξ_p , ξ_q as a function of real frequency ω_{Re} for pure case with $p = 0.55$, $q = 0.45$, $\varepsilon = 0.8$, $\varepsilon' = 0.2$. Note difference in scaling behaviour for p and q . Lines are provided as an aid to the eye.

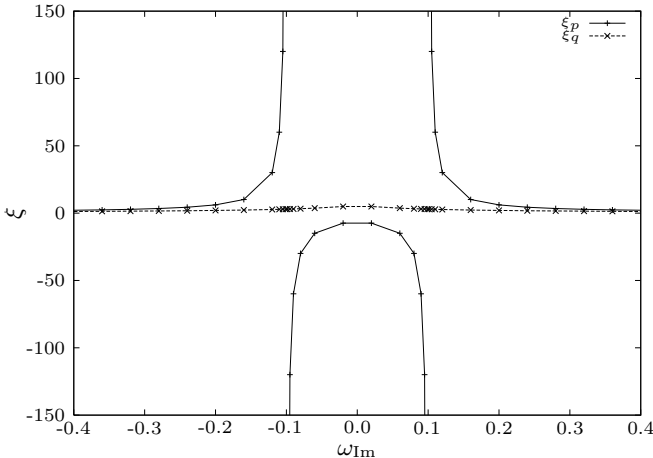


FIG. 8: Numerical localization lengths ξ_p , ξ_q as a function of complex frequency $\omega = 1 + i\omega_{\text{Im}}$ for pure case with $p = 0.55$, $q = 0.45$, $\varepsilon = 0.8$, $\varepsilon' = 0.2$. Note difference in scaling behaviour for p and q . Lines are provided as an aid to the eye.

and scales to the totally asymmetric case. So if we start with $p > q$, then p scales to infinity while q decays to zero.

In Figs. 7 and 8 we plot the localization lengths for p and q along the principal axes of the ω -space ellipse (again for the case $p > q$). As is evident from the discussion above, the localization length for q is small and positive in all regions— q is an irrelevant parameter under scaling. The localization length for p is positive in the localized region outside the ellipse, infinite on the allowed ellipse, and negative in the ballistic region inside (refer again to Fig. 5). The value of this relevant localization length can again be understood analytically by consider-

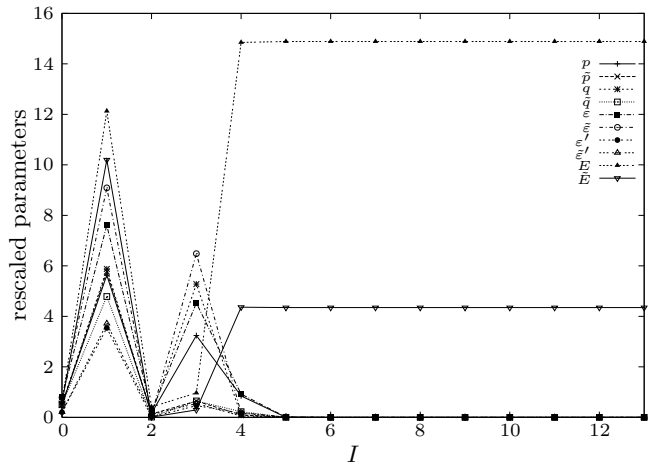


FIG. 9: Evolution of parameters in Eqs. (30) and (31) under $b = 2$ decimation. Disordered case with $\omega = 1.41$ and starting parameter values $p_{j,j-1} = \tilde{p}_{j-1,j} = q_{j-1,j} = \tilde{q}_{j,j-1} = 0.5$, $\varepsilon_{j,j-1} = \tilde{\varepsilon}_{j-1,j} = z$, $\varepsilon'_{j,j-1} = \tilde{\varepsilon}'_{j-1,j} = 1 - z$, $E = \tilde{E} = p_{j,j-1} - p_{j+1,j} - \varepsilon_{j+1,j} - \varepsilon'_{j,j-1}$ where z is a random variable drawn from a uniform distribution between 0.6 and 1.0. Graph shows absolute magnitude of parameters at site j_0 (averaged over 100 realizations of disorder) against number of iterations I ; lines are provided as an aid to the eye. Rate parameters decay exponentially as a function of 2^I showing a clear localization effect.

ing a complex wavevector in the dispersion relation.

C. Disordered model

Armed with this understanding of the pure case, we move on to look at the effect of disorder on the free-fermion system. There are obviously various different possible ways to add disorder; here we mainly investigate the case where the disorder is in ε and ε' with the rates chosen to maintain the free-fermion condition for each bond (specifically $\varepsilon'_j = 1 - \varepsilon_j$, $p_j = p$ and $q_j = q$, where $p+q = 1$). Once again, we consider in turn the symmetric ($p = q$) and asymmetric ($p \neq q$) cases.

1. Non-biased case, $p = q$

In Fig. 9 we show an example of the scaling behaviour for the case with $p_j = q_j = 0.5$, ε_j drawn from a uniform distribution and $\varepsilon'_j = 1 - \varepsilon_j$. The value of ω corresponds to being in the allowed band for the pure case (compare Fig. 2). We find that the rates evolve chaotically towards zero within an exponential envelope and so we can define a localization length via $r(l) \sim f(l)e^{-l/\xi}$. In Fig. 10 we plot the localization length for the decay of p , averaged over realizations of disorder. Localization is clearly seen for all values of ω in the pure band.

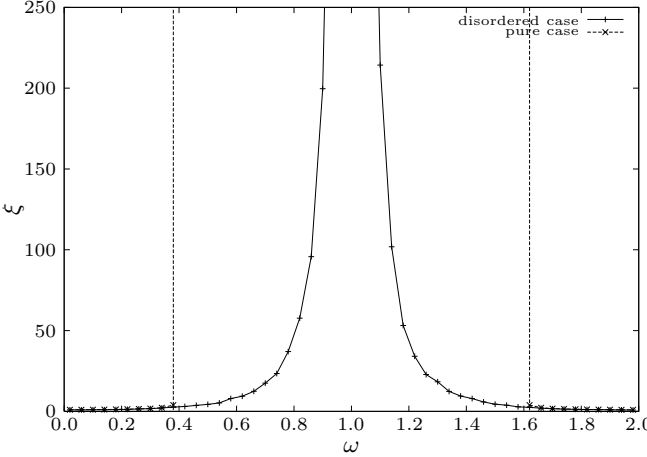


FIG. 10: Localization length for p scaling versus (real) frequency for disordered case with $p = q = 0.5$, $\varepsilon_j = z$, $\varepsilon'_j = 1 - z$ where z is drawn from a uniform distribution between 0.6 and 1.0. Pure results outside the band are also shown for comparison (dashed). In the disordered case, the localization length is finite everywhere except $\omega = 1$.

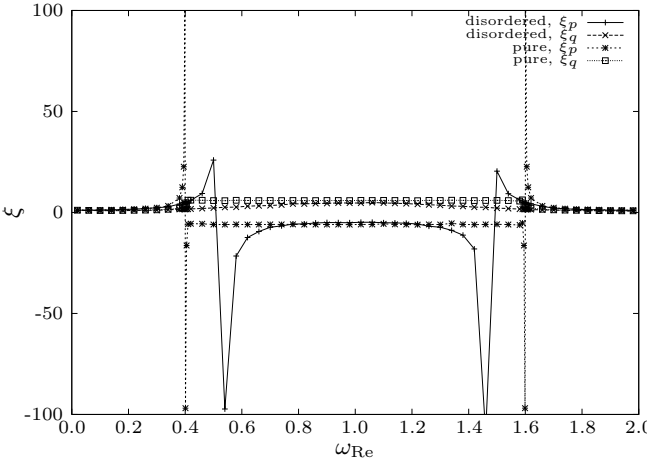


FIG. 11: Numerical localization lengths ξ_p , ξ_q as a function of real frequency ω_{Re} for disordered case with $p = 0.55$, $q = 0.45$, $\varepsilon_j = z$, $\varepsilon'_j = 1 - z$ where z is drawn from a uniform distribution between 0.6 and 1.0. Lines are provided as an aid to the eye. Pure results are shown for comparison. Note the reduction of the ballistic region in the disordered case.

2. Biased case, $p \neq q$

In Fig. 11 we plot the localization lengths for p and q along the real frequency axis for a sample disordered case, viz., $p_j = 0.55$, $q_j = 0.45$, ε_j drawn from a uniform distribution and $\varepsilon'_j = 1 - \varepsilon_j$. The pure results are also shown for reference (compare also Fig. 7). In this case we see that disorder reduces the size of the allowed ellipse along the real- ω axis, i.e., it acts to increase the localized region at the expense of the ballistic region. The results

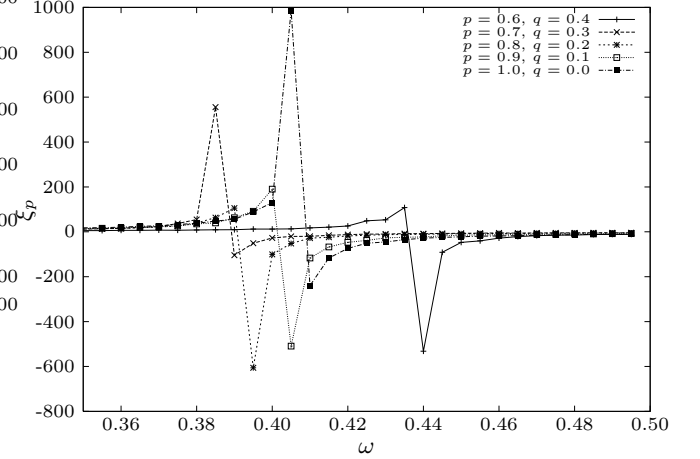


FIG. 12: Numerical localization length ξ_p as a function of real frequency ω_{Re} for disordered cases with $\varepsilon_j = z$, $\varepsilon'_j = 1 - z$ where z is drawn from a uniform distribution between 0.6 and 1.0. Results are shown for a range of values of p and q as indicated by the legend. Lines are provided as an aid to the eye.

for $\omega = 1 + i\omega_{\text{Im}}$ are essentially the same as in the pure case (Fig. 8).

This competition between disorder-induced localization and driving is analogous to that arising in another non-Hermitian Hamiltonian studied by Hatano and Nelson [33]. Their work was motivated by the mapping between flux lines in a $(d+1)$ -dimensional superconductor and d -dimensional bosons. A random potential in the bosonic problem arises from the study of columnar defects in the superconductor.

For all cases with disorder only in ε and ε' , we find that the localization length is altered along the real- ω axis but unchanged along the axis in the imaginary direction.² However, the change in the position of the allowed band (where the localization length is infinite) depends on the strength of the driving $p - q$, see Fig. 12. We shall now consider some tentative analytical ideas to quantify these disorder effects.

Recall that the pure spectrum is given by

$$\lambda_k = b_0 - a_0 \cos k + i(p - q) \sin k, \quad (33)$$

with $b_0 = \varepsilon' + \varepsilon$ and $a_0 = \varepsilon' - \varepsilon$. We seek to modify this to represent the effective spectrum of the disordered model. For the case of disordered ε and ε' (with $\varepsilon_j + \varepsilon'_j = p + q = 1$) then a naive suggestion is

$$\lambda_k = b_0 - a \cos k + i(p - q) \sin k \quad (34)$$

where a can, in principle, have both real and imaginary

² Obviously disorder in p and q affects the imaginary- ω direction instead.

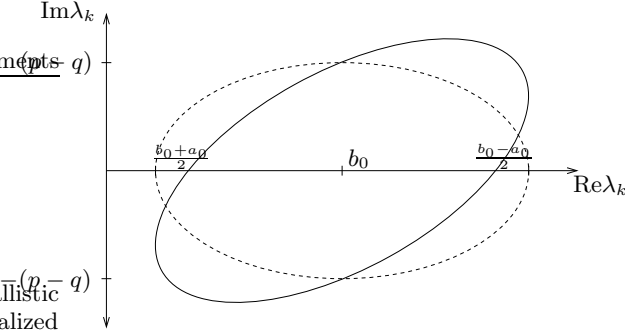


FIG. 13: Schematic of effective disordered dispersion relation in ω -space for $\lambda_k = b_0 + (a_0 + i2\delta) \cos k + i(p - q) \sin k$ (solid line). Pure case $\lambda_k = b_0 + a_0 \cos k + i(p - q) \sin k$ is shown for comparison (dashed line). Inside the ellipse equations of motion scale to ballistic limit $p/q \rightarrow \infty$; outside of ellipse is localized region.

parts, i.e.,

$$a = \tilde{a} + i2\delta \quad (35)$$

with \tilde{a}, δ real. The imaginary part of a causes a rotation of the allowed ellipse (see Fig. 13); if $\tilde{a} \neq a_0$, then there is also stretching or compression. In agreement with the numerical localization length data, this form leaves the centre of the ellipse and the intersection with the $\omega = b_0$ axis unchanged. It also explains why any amount of disorder causes localization in the $p = q$ case (where the ellipse is a line along the real axis) for all values of real frequency except $\omega = 1$.

There is no *a priori* reason why the imaginary part of a should have a positive sign so we naturally expect the possibility of both $\pm 2\delta$. Furthermore, we anticipate that \tilde{a} is related to the mean of $\varepsilon' - \varepsilon$ and δ is proportional to the width of the distribution. In fact, comparisons of the obtained localization lengths (e.g., see Fig. 12) with the prediction from the dispersion relation (34) suggest that the scaling results can not be described by unique values of \tilde{a}, δ . It appears that what we measure in the numerical scaling procedure, is the average of $1/\xi$ for some range of values. Further work is needed to check and quantify this hypothesis.

V. DISORDER EFFECTS IN STOCHASTIC SYSTEM

In this section we attempt to infer disorder effects in the original stochastic hopping process by mapping back the results for the equivalent quantum free-fermion model. In particular, we are interested in disorder-induced changes to the pure steady-state density (11).

We argue from the previous section that one can crudely characterize the effects of disorder in the evaporation-deposition rates by the replacements $\varepsilon' \rightarrow \varepsilon' \pm i\delta$, $\varepsilon \rightarrow \varepsilon \mp i\delta$ ($a_0 \rightarrow a_0 \pm i2\delta$) where δ is related

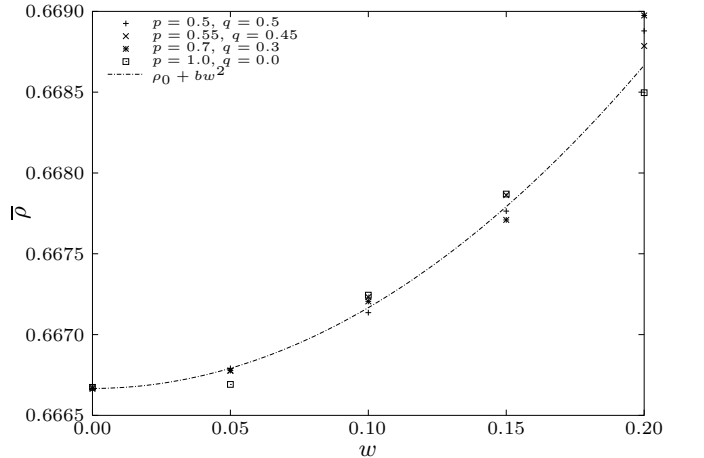


FIG. 14: Simulation results showing density dependence on width of $\varepsilon, \varepsilon'$ distribution for range of p, q values (see legend) in a system of size 1000. ε_j is drawn from a uniform distribution between $0.8 - w$ and $0.8 + w$; ε'_j given by $1 - \varepsilon_j$. Dashed line is a squared fit given by $\bar{\rho} = \rho_0 + bw^2$ with $b = 0.05$.

to the width of the disorder distribution. This gives two different effective Bogoliubov angles (possibly connected to the doubling of fermionic degrees of freedom in the work of Merz and Chalker [31]). Stochastic observables are presumably related to the average of these two possibilities but it is not yet clear what is the appropriate function of $\varepsilon, \varepsilon'$ to average over. Motivated by the form of the Bogoliubov transformation [cf. Eqs. (24) and (25)] and by comparisons with simulation, we suggest that the ratio ε'/ε is the important quantity and hence define

$$\overline{\left(\frac{\varepsilon'}{\varepsilon}\right)} = \frac{1}{2} \left(\frac{\varepsilon' + i\delta}{\varepsilon - i\delta} + \frac{\varepsilon' - i\delta}{\varepsilon + i\delta} \right). \quad (36)$$

This then yields a disorder-averaged density

$$\overline{\rho_l} = \frac{1}{1 + \sqrt{(\varepsilon'/\varepsilon)}}, \quad (37)$$

which is increased from the pure case by an amount proportional to δ^2 (for small δ). Simulations on the stochastic model (see Fig. 14) confirm a density shift proportional to the square of the width of the distribution, i.e., the localization in the disordered free-fermion model does appear to map back to a density shift in the equivalent disordered stochastic system. Further work is still needed to rigorously establish this picture and to relate the value of δ both to the details of the disorder distribution and to the numerical localization data.

Similarly, from knowledge of the effective dispersion relation for the disordered case, it should be possible to adapt the pure treatment of [22] for both steady-state dynamic correlation functions and non-steady-state properties. These quantities typically contain time-dependences of the form $e^{-Re\lambda_k t}$ so any decrease in the effective spec-

tral gap would be expected to lead to a slowing-down of the dynamics (as was found for the ASEP in [11]).

VI. DISCUSSION

In this paper we have studied the effect of disorder on a model consisting of the partially asymmetric exclusion process combined with dimer evaporation-deposition. We presented an exact mapping to an equivalent quantum system and then employed a numerical scaling technique on the quantum equations of motion. This provided a clear demonstration of disorder-induced localization acting in competition with the asymmetric driving. We discussed tentatively how these localization effects are related to the observed steady-state density shift in the original stochastic system; exact details of the inverse transformation remain to be clarified. The stochastic system is relatively robust to disorder since particle pairs can be evaporated/deposited along the whole length of the chain.

There is much scope for further work on this disordered model. In particular, a more rigorous development of the mapping from the disordered quantum model back

to the stochastic system is needed. This would permit the translation of numerical scaling results for different forms of disorder (including, for example, the case where all rates are disordered and $\varepsilon_j + \varepsilon'_j = p_j + q_j$ is position-dependent) into quantitative statements about the effect on density and correlation functions. As indicated at the end of Sec. V we should also like to extend the discussion to dynamics.

Acknowledgments

We would like to thank John Chalker for helpful discussions. This work was supported by EPSRC under Oxford Condensed Matter Theory Grants GR/R83712/01 and GR/M04426/01 together with Grant No. 309261.

APPENDIX A: DISORDERED FREE-FERMION SCALING

Here we present scaling relations for the coupled free-fermion equations of motion (30) and (31):

$$(E_j - \omega)\Gamma_j = -p_{j,j-1}\Gamma_{j-1} - q_{j,j+1}\Gamma_{j+1} + \varepsilon_{j,j-1}\gamma_{j-1} - \tilde{\varepsilon}_{j,j+1}\gamma_{j+1}, \quad (A1)$$

$$(\tilde{E}_j + \omega)\gamma_j = -\tilde{p}_{j,j+1}\gamma_{j+1} - \tilde{q}_{j,j-1}\gamma_{j-1} + \varepsilon'_{j,j-1}\Gamma_{j-1} - \tilde{\varepsilon}'_{j,j+1}\Gamma_{j+1}. \quad (A2)$$

A $b = 2$ decimation of these equations leads to

$$(E'_j - \omega)\Gamma_j = -p'_{j,j-2}\Gamma_{j-2} - q'_{j,j+2}\Gamma_{j+2} + (\varepsilon)'_{j,j-2}\gamma_{j-2} - (\tilde{\varepsilon})'_{j,j+2}\gamma_{j+2}, \quad (A3)$$

$$(\tilde{E}'_j + \omega)\gamma_j = -\tilde{p}'_{j,j+2}\gamma_{j+2} - \tilde{q}'_{j,j-2}\gamma_{j-2} + (\varepsilon')'_{j,j-2}\Gamma_{j-2} - (\tilde{\varepsilon}')'_{j,j+2}\Gamma_{j+2}, \quad (A4)$$

with rescaled “energy” parameters

$$E'_j = E_j - \frac{p_{j,j-1}q_{j-1,j}}{E_{j-1} - \omega} - \frac{q_{j,j+1}p_{j+1,j}}{E_{j+1} - \omega} + \frac{\varepsilon_{j,j-1}\tilde{\varepsilon}'_{j-1,j}}{\tilde{E}_{j-1} + \omega} + \frac{\tilde{\varepsilon}_{j,j+1}\varepsilon'_{j+1,j}}{\tilde{E}_{j+1} + \omega}, \quad (A5)$$

$$\tilde{E}'_j = \tilde{E}_j - \frac{\tilde{q}_{j,j-1}\tilde{p}_{j-1,j}}{\tilde{E}_{j-1} + \omega} - \frac{\tilde{p}_{j,j+1}\tilde{q}_{j+1,j}}{\tilde{E}_{j+1} + \omega} + \frac{\varepsilon'_{j,j-1}\tilde{\varepsilon}_{j-1,j}}{E_{j-1} - \omega} + \frac{\tilde{\varepsilon}'_{j,j+1}\varepsilon_{j+1,j}}{E_{j+1} - \omega}, \quad (A6)$$

and the rescaled rates

$$p'_{j,j-2} = \frac{-\left(\frac{p_{j,j-1}p_{j-1,j-2}}{E_{j-1}-\omega} + \frac{\varepsilon_{j,j-1}\varepsilon'_{j-1,j-2}}{\bar{E}_{j-1}+\omega}\right) + \frac{A_j}{\bar{E}'_j+\omega}\left(\frac{\varepsilon_{j,j-1}p_{j-1,j-2}}{E_{j-1}-\omega} + \frac{\bar{q}_{j,j-1}\varepsilon'_{j-1,j-2}}{\bar{E}_{j-1}+\omega}\right)}{1 - \frac{A_j B_j}{(E'_j - \omega)(\bar{E}'_j + \omega)}}, \quad (\text{A7})$$

$$q'_{j,j+2} = \frac{-\left(\frac{q_{j,j+1}q_{j+1,j+2}}{E_{j+1}-\omega} + \frac{\tilde{\varepsilon}_{j,j+1}\tilde{\varepsilon}'_{j+1,j+2}}{\tilde{E}_{j+1}+\omega}\right) - \frac{A_j}{\tilde{E}'_j+\omega}\left(\frac{\tilde{\varepsilon}'_{j,j+1}q_{j+1,j+2}}{E_{j+1}-\omega} + \frac{\tilde{p}_{j,j+1}\tilde{\varepsilon}'_{j+1,j+2}}{\tilde{E}_{j+1}+\omega}\right)}{1 - \frac{A_j B_j}{(\tilde{E}'_j - \omega)(\tilde{E}'_j + \omega)}}, \quad (\text{A8})$$

$$(\varepsilon')_{j,j-2} = \frac{-\left(\frac{p_{j,j-1}\varepsilon_{j-1,j-2}}{E_{j-1}-\omega} + \frac{\varepsilon_{j,j-1}\tilde{q}_{j-1,j-2}}{\tilde{E}_{j-1}+\omega}\right) + \frac{A_j}{\tilde{E}'_j+\omega}\left(\frac{\varepsilon'_{j,j-1}\varepsilon_{j-1,j-2}}{E_{j-1}-\omega} + \frac{\tilde{q}_{j,j-1}\tilde{q}_{j-1,j-2}}{\tilde{E}_{j-1}+\omega}\right)}{1 - \frac{A_j B_j}{(\tilde{E}'_j-\omega)(\tilde{E}'_j+\omega)}}, \quad (\text{A9})$$

$$(\tilde{\varepsilon})'_{j,j+2} = \frac{-\left(\frac{q_{j,j+1}\tilde{\varepsilon}_{j+1,j+2}}{E_{j+1}-\omega} + \frac{\tilde{\varepsilon}_{j,j+1}\tilde{p}_{j+1,j+2}}{\tilde{E}_{j+1}+\omega}\right) - \frac{A_j}{E'_j+\omega}\left(\frac{\tilde{\varepsilon}'_{j,j+1}\tilde{\varepsilon}_{j+1,j+2}}{E_{j+1}-\omega} + \frac{\tilde{p}_{j,j+1}\tilde{p}_{j+1,j+2}}{\tilde{E}_{j+1}+\omega}\right)}{1 - \frac{A_j B_j}{(E'_j-\omega)(E'_j+\omega)}}, \quad (\text{A10})$$

$$\tilde{p}'_{j,j+2} = \frac{-\left(\frac{\tilde{\varepsilon}'_{j,j+1}\tilde{\varepsilon}_{j+1,j+2}}{E_{j+1}-\omega} + \frac{\tilde{p}_{j,j+1}\tilde{p}_{j+1,j+2}}{E_{j+1}+\omega}\right) - \frac{B_j}{E'_j+\omega}\left(\frac{q_{j,j+1}\tilde{\varepsilon}_{j+1,j+2}}{E_{j+1}-\omega} + \frac{\tilde{\varepsilon}_{j,j+1}\tilde{p}_{j+1,j+2}}{E_{j+1}+\omega}\right)}{1 - \frac{A_j B_j}{(E'_j-\omega)(E'_j+\omega)}}, \quad (\text{A11})$$

$$\tilde{q}'_{j,j-2} = \frac{-\left(\frac{\varepsilon'_{j,j-1}\varepsilon_{j-1,j-2}}{E_{j-1}-\omega} + \frac{\tilde{q}_{j,j-1}\tilde{q}_{j-1,j-2}}{\tilde{E}_{j-1}+\omega}\right) + \frac{B_j}{E'_j+\omega}\left(\frac{p_{j,j-1}\varepsilon_{j-1,j-2}}{E_{j-1}-\omega} + \frac{\varepsilon_{j,j-1}\tilde{q}_{j-1,j-2}}{\tilde{E}_{j-1}+\omega}\right)}{1 - \frac{A_j B_j}{(E'_j-\omega)(E'_j+\omega)}}, \quad (\text{A12})$$

$$(\varepsilon')_{j,j-2}' = \frac{-\left(\frac{\varepsilon'_{j,j-1}p_{j-1,j-2}}{E_{j-1}-\omega} + \frac{\tilde{q}_{j,j-1}\varepsilon'_{j-1,j-2}}{\tilde{E}_{j-1}+\omega}\right) + \frac{B_j}{E'_j+\omega} \left(\frac{p_{j,j-1}p_{j-1,j-2}}{E_{j-1}-\omega} + \frac{\varepsilon_{j,j-1}\varepsilon'_{j-1,j-2}}{\tilde{E}_{j-1}+\omega}\right)}{1 - \frac{A_j B_j}{(E'_j-\omega)(E'_j+\omega)}}, \quad (\text{A13})$$

$$(\tilde{\varepsilon}')_{j,j+2}' = \frac{-\left(\frac{\tilde{\varepsilon}'_{j,j+1}q_{j+1,j+2}}{E_{j+1}-\omega} + \frac{\tilde{p}_{j,j+1}\tilde{\varepsilon}'_{j+1,j+2}}{E_{j+1}+\omega}\right) - \frac{B_j}{E'_j+\omega} \left(\frac{q_{j,j+1}q_{j+1,j+2}}{E_{j+1}-\omega} + \frac{\tilde{\varepsilon}'_{j,j+1}\tilde{\varepsilon}'_{j+1,j+2}}{E_{j+1}+\omega}\right)}{1 - \frac{A_j B_j}{(E'_j-\omega)(E'_j+\omega)}} \quad (\text{A14})$$

$$\begin{pmatrix} p_{i,i-1} \tilde{\varepsilon}_{i-1,i} & q_{i,i+1} \varepsilon_{i+1,i} & \varepsilon_{i,i-1} \tilde{p}_{i-1,i} & \tilde{\varepsilon}_{i,i+1} \tilde{q}_{i+1,i} \end{pmatrix} \quad (A.15)$$

where

$$A_j = \left(\frac{p_{j,j-1} \tilde{\varepsilon}_{j-1,j}}{E_{j-1} - \omega} - \frac{q_{j,j+1} \varepsilon_{j+1,j}}{E_{j+1} - \omega} - \frac{\varepsilon_{j,j-1} \tilde{p}_{j-1,j}}{\tilde{E}_{j-1} + \omega} + \frac{\tilde{\varepsilon}_{j,j+1} \tilde{q}_{j+1,j}}{\tilde{E}_{j+1} + \omega} \right), \quad (\text{A15})$$

$$B_j = \left(-\frac{\varepsilon'_{j,j-1} q_{j-1,j}}{E_{j-1} - \omega} + \frac{\tilde{\varepsilon}'_{j,j+1} p_{j+1,j}}{E_{j+1} - \omega} + \frac{\tilde{q}_{j,j-1} \tilde{\varepsilon}'_{j-1,j}}{\tilde{E}_{j-1} + \omega} - \frac{\tilde{p}_{j,j+1} \varepsilon'_{j+1,j}}{\tilde{E}_{j+1} + \omega} \right). \quad (\text{A16})$$

Note the difference in meaning between ε' (the evaporation rate) and $(\varepsilon)'$ (the scaled deposition rate).

- [1] B. Schmittmann and R. K. P. Zia, in *Phase Transitions and Critical Phenomena*, edited by C. Domb and J. Lebowitz (Academic Press, 1995), vol. 17.
- [2] G. Tripathy and M. Barma, Phys. Rev. E **58**, 1911 (1998).
- [3] M. Lässig, J. Phys.: Condens. Matter **10**, 9905 (1998).
- [4] R. B. Stinchcombe, J. Phys.: Condens. Matter **14**, 1473 (2002).
- [5] M. R. Evans, T. Hanney, and Y. Kafri, Phys. Rev. E **70**, 066124 (2004).
- [6] J. Krug and P. A. Ferrari, J. Phys. A: Math. Gen. **29**, L465 (1996).
- [7] M. R. Evans, Europhys. Lett. **36**, 13 (1996).
- [8] K. Jain and M. Barma, Phys. Rev. Lett. **91**, 135701 (2003).
- [9] J. Krug, Braz. J. Phys. **30**, 97 (2000).
- [10] K. M. Kolwankar and A. Punnoose, Phys. Rev. E **61**, 2453 (2000).
- [11] R. J. Harris and R. B. Stinchcombe, Phys. Rev. E **70**, 016108 (2004).
- [12] M. D. Grynb erg and R. B. Stinchcombe, Phys. Rev. Lett. **74**, 1242 (1995).
- [13] M. D. Grynb erg and R. B. Stinchcombe, Phys. Rev. Lett. **76**, 851 (1996).

- [14] J. E. Santos, J. Phys. A: Math. Gen. **30**, 3249 (1997).
- [15] F. C. Alcaraz and V. Rittenberg, Phys. Lett. B **314**, 377 (1993).
- [16] I. Peschel, V. Rittenberg, and U. Schultze, Nucl. Phys. B **430**, 633 (1994).
- [17] I. R. Pimentel and R. B. Stinchcombe, Europhys. Lett. **6**, 719 (1988).
- [18] P. Jordan and E. Wigner, Z. Phys. **47**, 631 (1928).
- [19] N. N. Bogoliubov, Nuovo Cimento **7**, 794 (1958).
- [20] J. G. Valatin, Nuovo Cimento **7**, 843 (1958).
- [21] F. C. Alcaraz, M. Droz, M. Henkel, and V. Rittenberg, Ann. Phys. (N.Y.) **230**, 250 (1994).
- [22] M. D. Grynberg, T. J. Newman, and R. B. Stinchcombe, Phys. Rev. E **50**, 957 (1994).
- [23] M. Henkel, E. Orlandini, and G. M. Schütz, J. Phys. A: Math. Gen. **28**, 6335 (1995).
- [24] R. Kroon, H. Fleurent, and R. Sprak, Phys. Rev. E **47**, 2462 (1993).
- [25] G. M. Schütz, in *Phase Transitions and Critical Phenomena*, edited by C. Domb and J. Lebowitz (Academic Press, London, 2001), vol. 19.
- [26] J. Santos, G. M. Schütz, and R. B. Stinchcombe, J. Chem. Phys. **105**, 2399 (1996).
- [27] R. J. Glauber, J. Math. Phys. **4**, 294 (1963).
- [28] F. Family and J. G. Amar, J. Stat. Phys. **65**, 1235 (1991).
- [29] N.-N. Chen and R. B. Stinchcombe, Phys. Rev. E **49**, 2784 (1994).
- [30] M. D. Grynberg and R. B. Stinchcombe, Phys. Rev. E **61**, 324 (2000).
- [31] F. Merz and J. T. Chalker, Phys. Rev. B **65**, 054425 (2002).
- [32] J. M. Ziman, *Models of disorder* (CUP, Cambridge, 1979), chap. 8.
- [33] N. Hatano and D. R. Nelson, Phys. Rev. Lett. **77**, 570 (1996).